

Quercetin-Loaded Nanoparticles: A Promising Therapeutic Strategy for Inflammatory Bowel Disease

Wenpeng Wang^{1,2,*}, Mingrui Li^{1,3,*}, Ying Liu^{1,*}, Benno Weigmann^{1,4}

¹Medical Clinic I, Kussmaul Campus for Medical Research, University of Erlangen-Nürnberg, Erlangen, Germany; ²Department of Colorectal Oncology, Tianjin Medical University Cancer Institute and Hospital, National Clinical Research Center for Cancer, Tianjin's Clinical Research Center for Cancer, Tianjin Key Laboratory of Digestive Cancer, Tianjin, People's Republic of China; ³Department of Endocrinology, Dazhou Central Hospital, Dazhou, People's Republic of China; ⁴FAU Profile Center Immunomedicine, University of Erlangen-Nürnberg, Erlangen, Germany

*These authors contributed equally to this work

Correspondence: Benno Weigmann, Medical Clinic I, Kussmaul Campus for Medical Research, University of Erlangen-Nürnberg, Hartmannstr.14, Erlangen, 91052, Germany, Tel +49 9131 85-35885, Fax +49 9131 85-355959, Email benno.weigmann@uk-erlangen.de

Purpose: The aim of this study was to evaluate the characteristics and therapeutic efficacy of quercetin-loaded nanoparticles (NPs) using poly lactic-co-glycolic acid (PLGA) and Eudragit S100 (ES100) as carriers in the treatment of inflammatory bowel disease (IBD).

Materials and Methods: Quercetin-loaded NPs were prepared using PLGA (QU-PLGA) and a combination of PLGA and ES100 (QU-PE). The mean particle sizes, encapsulation efficiencies, and stability of quercetin in aqueous solutions were assessed. Drug release profiles were evaluated under different pH conditions. In vitro studies involved cell endocytosis and cytotoxicity assays using Caco-2 and SW480 cells. In vivo efficacy was tested in dextran sulfate sodium (DSS) and oxazolone (OXA) induced acute colitis models in mice, with assessments including weight retention, colonic length, Murine Endoscopic Index of Colitis Severity (MEICS), histological scores, and inflammatory markers.

Results: Quercetin-loaded NPs (QU-PLGA: 160.4 ± 3.68 nm; QU-PE: 161.0 ± 2.30 nm) exhibited significantly smaller particle sizes compared to free quercetin (QU-Free: 2239 ± 404 nm) and high encapsulation efficiencies (87–90%). QU-PE showed pH-dependent release with improved stability in aqueous solutions. Quercetin-loaded NPs demonstrated enhanced cell membrane penetration and were non-toxic at tested concentrations. In the DSS and OXA colitis models, quercetin-loaded NPs significantly reduced disease severity, as evidenced by improved weight retention, longer colonic length, reduced MEICS and histological scores, decreased pro-inflammatory cytokines, and higher E-Cadherin expression compared to untreated groups. Notably, QU-PE demonstrated consistent anti-inflammatory effects across both models, with particularly pronounced efficacy in OXA-induced colitis, while QU-PLGA showed relatively superior therapeutic performance in the DSS model.

Conclusion: Quercetin-loaded NPs enhance the stability, bioavailability, and therapeutic efficacy of quercetin in IBD, offering a promising therapeutic strategy with superior physiological relevance for colitis treatment.

Keywords: quercetin, nanoparticles, poly lactic-co-glycolic acid, PLGA, Eudragit S100, inflammatory bowel disease, therapeutic efficacy

Introduction

Inflammatory bowel disease (IBD) is a group of chronic inflammatory conditions of the gastrointestinal tract, primarily including Crohn's disease and ulcerative colitis (UC).¹ The pathogenesis of IBD involves a complex interplay of genetic, environmental, and immunological factors, leading to a dysregulated immune response and chronic intestinal inflammation.^{1,2} Traditional treatments for IBD focus on controlling inflammation and sustaining remission, but they often present considerable side effects and exhibit inconsistent effectiveness.

Quercetin, a natural flavonoid found in many fruits and vegetables, has garnered attention for its potent anti-inflammatory, antioxidant, and immunomodulatory properties.^{3,4} The therapeutic potential of quercetin in IBD merits comprehensive examination, given its pleiotropic mechanisms of action. Emerging evidence indicates that this bioactive flavonoid exerts multifaceted protection against IBD pathogenesis through interconnected pathways. For instance, quercetin downregulates pro-inflammatory cytokines (TNF- α , IL-6) involved in immune hyperactivation by inhibiting PI3K and AKT signaling.⁵ It can activate the Nrf2 antioxidant pathway, reducing oxidative stress in intestinal epithelium.⁶ Furthermore, it modulates gut microbial composition, enhancing beneficial bacterial genera like *Adlercreutzia* and *Photobacterium* while inhibiting pathogenic species.^{5,7} It also strengthens intestinal barrier integrity through upregulation of tight junction proteins such as occludin, illustrating its comprehensive approach to IBD management by targeting multiple disease-relevant pathways simultaneously.⁵ However, its therapeutic application in IBD is limited by its poor bioavailability and rapid degradation in the gastrointestinal environment.⁸ To overcome these challenges, novel drug delivery systems are being explored to enhance the stability, bioavailability, and targeted delivery of quercetin.

One promising approach involves the use of biodegradable polymers such as poly lactic-co-glycolic acid (PLGA) or Eudragit S100 (ES100) to encapsulate quercetin. PLGA, a well-established biocompatible and biodegradable polymer, provides sustained drug release and protects the encapsulated agent from premature degradation.⁹ ES100, a pH-sensitive polymer, allows for targeted drug release in the colon, where the inflammation is most pronounced in IBD patients.¹⁰ Notably, no prior studies have investigated quercetin encapsulated in both PLGA and ES100 (QU-PE) for IBD treatment, despite the success of similar systems (eg, garcinol-PLGA/ES100) in reducing inflammation and promoting mucosal healing in preclinical models.¹¹ By combining these two polymers, a dual-encapsulation system may be developed to enhance the therapeutic efficacy of quercetin in treating IBD. This innovative drug delivery system offers a promising strategy to improve the clinical management of IBD by maximizing the therapeutic benefits of quercetin while minimizing its drawbacks. This study aims to provide an overview of the potential of quercetin encapsulated in PLGA (QU-PLGA) or QU-PE as a novel therapeutic approach for IBD.

Materials and Methods

Preparation of QU-PLGA and QU-PE

Quercetin-loaded NPs were prepared using the nanoprecipitation method. For QU-PLGA NPs, 2.5 mg of quercetin (Sigma-Aldrich, USA) and 15 mg of PLGA (Thermo Fisher Scientific, USA) were dissolved in 1000 μ L of acetone and added dropwise to 10 mL of 1% polyvinyl alcohol (PVA, Carl-Roth, Germany) solution, stirred at 1500 rpm overnight. The mixture was sonicated for 10 minutes on ice, then centrifuged at 15,000 rpm for 30 minutes. The supernatant was discarded, and the pellet was washed three times with 1000 μ L of Millipore water, each wash followed by centrifugation at 15,000 rpm for 5 minutes. The final pellet was resuspended in 1000 μ L of Millipore water and vortexed until fully dispersed, then stored at 4°C. For QU-PE NPs, 2.5 mg of quercetin, 15 mg of PLGA, and 15 mg of ES100 (Evonik, Germany) were dissolved in 1000 μ L of acetone. The remaining procedures were the same as for the PLGA NPs.

Size and Zeta Potential of NPs

Quercetin-loaded NPs and QU-Free were analyzed for size and zeta potential using a Zetasizer2000HS (Malvern Instruments, UK) with dynamic light scattering (DLS). Both size and zeta potential measurements were done in triplicate at room temperature. Results were reported as mean \pm standard deviation (SD).

Encapsulation Efficiency (EE)

EE of quercetin was determined by dissolving 100 μ L of NPs suspension in 900 μ L of acetone and shaking for 4 hours at room temperature to fully extract quercetin. The mixture was then centrifuged at 15,000 rpm for 5 minutes, and the supernatant was collected. To measure quercetin concentration, 20 μ L of the supernatant was diluted in 980 μ L of methanol, and absorbance was recorded at 337 nm using an enzyme linked immunosorbent assay (ELISA) Reader InfiniteM200 (Tecan, Switzerland). A standard curve (0–10 μ g/mL) was prepared under the same conditions. EE was

calculated using the formula: $EE (\%) = [\text{quercetin (encapsulated)} / \text{quercetin (total)}] \times 100$. The absorption peak of quercetin was confirmed by scanning its methanol solutions.

Morphology of Quercetin-Loaded NPs

Staff at the Department of Materials Science, Friedrich-Alexander-Universität Erlangen-Nürnberg (FAU), assisted us with NPs morphology imaging using scanning electron microscopy (SEM, Merlin, Zeiss, Germany).

In vitro Drug Release

Quercetin, due to its poor solubility in water, was quantified following its release from NPs. To simulate NPs degradation under cell culture conditions, 1 mL of NPs suspension was mixed with 9 mL of phosphate-buffered saline (PBS, pH 7.3). This mixture was distributed into 10 centrifuge tubes (1 mL each) and incubated at 37°C with 5% CO₂ for 24 hours. At regular intervals, 2 tubes were removed, centrifuged at 15,000 rpm and 4°C for 10 minutes, and the pelleted quercetin was dissolved in 1 mL of methanol. Absorbance at 337 nm was measured by ELISA, and the quercetin concentration was determined based on a standard curve in methanol. The release rate of quercetin was calculated using the formula: $\text{Release rate (\%)} = [\text{quercetin (released)} / \text{quercetin (total)}] \times 100$.

Simulated gastric fluid (SGF, pH 1.2) and simulated intestinal fluid (SIF, pH 7.4) were also used to replicate gastrointestinal conditions. For this, 1 mL of NPs suspension was dispersed in 9 mL of SIF, and the same procedure was followed.

Fluorescently Tagged NPs and QU-Free

Coumarin 6 (Sigma-Aldrich, USA), a fluorescent dye, was utilized to label NPs and QU-Free. For coumarin 6-labeled QU-PLGA, 2.5 mg of quercetin and 0.25 mg of coumarin 6 were dissolved in 1 mL of acetone containing 15 mg of PLGA at room temperature. The mixture was then processed according to the standard QU-PLGA production procedure.

For coumarin 6-labeled QU-PE, 500 μL of acetone containing 2.5 mg of quercetin and 0.5 mg of coumarin 6 was combined with 1 mL of acetone solution containing 15 mg of PLGA and 15 mg of ES100. The subsequent steps followed the same protocol as for QU-PLGA.

To label QU-Free with coumarin 6, quercetin was dissolved in 10 mL of stirring Millipore water. Then, 1 mL of ethanol containing coumarin 6 was added dropwise. The mixture was stirred at 500 rpm for 4 hours at room temperature. Excess ethanol and water were removed by centrifugation at 15,000 rpm for 10 minutes. The pellet was resuspended in Millipore water, washed 3 times, and stored at 4°C. The weight ratio of coumarin 6 to quercetin was 1:10.

Cell Experiments

Cell Culture

Two cell lines, Caco-2 and SW480, were sourced from the European Collection of Authenticated Cell Cultures (ECACC) and maintained in complete RPMI-1640 medium (Thermo Fisher Scientific, USA), which was enhanced with 10% fetal bovine serum (FBS) (Sigma-Aldrich, USA), penicillin (100 U/mL), and streptomycin (0.1 mg/mL) (Sigma-Aldrich, USA). These cells were incubated at 37°C with 5% CO₂.

Cytotoxicity Assay

The cytotoxicity of quercetin-loaded NPs was assessed on Caco-2 and SW480 cell lines using MTT (Sigma-Aldrich, USA) assay. In short, 100 μL of complete RPMI 1640 medium, containing Caco-2 cells at a density of 1×10^5 cells/mL, were plated into 96-well plates. Following a 24-hour incubation period, the medium was discarded, and Caco-2 cells were treated with fresh medium without FBS, containing different concentrations of drug (0, 1, 2, 5, 10, 20, 40 μM). After 24 hours of drug exposure, the medium was removed, and the cells were washed 3 times with PBS. Subsequently, the Caco-2 cells were incubated for 4 hours with 0.5 mg/mL MTT solution in medium (100 μL) without FBS. After the medium was discarded, the purple formazan crystals were dissolved in 100 μL of dimethyl sulfoxide (DMSO, Merck, Germany) for 10 minutes. Absorbance was then measured at 550 nm using an ELISA reader. All experiments were conducted in triplicate and recorded. The procedure for SW480 cells was identical to that of Caco-2 cells.

Permeability Study of NPs

Transepithelial electrical resistance (TEER) is commonly used as an initial indicator for assessing the permeability of tight junctions. In this study, Caco-2 cells were seeded at a density of 50,000 cells/mL onto 24-well inserts and cultured in complete RPMI 1640 medium for 21 days, with the medium changed twice per week. TEER values were measured at room temperature using electrodes connected to an epithelial voltohm meter, with the chopstick electrodes placed in both chambers of each Transwell insert. The TEER value was calculated using the following formula: TEER value ($\Omega \cdot \text{cm}^2$) = (total TEER – blank TEER) (Ω) \times Area (cm^2).

For the permeability study of NPs, only Caco-2 cell monolayers that had been cultured for 21 days and had TEER values above 400 $\Omega \cdot \text{cm}^2$ were selected. These Caco-2 cells were then incubated for 4 hours at 37°C with fluorescently labelled quercetin and its NPs solutions, where PLGA or PE-loaded NPs solutions contained a quercetin concentration of 10 μM . These solutions were prepared using culture medium without FBS. After 4-hour incubation, the medium was removed, and Caco-2 cell monolayers were fixed with 100 μL of 4.5% paraformaldehyde (PFA, Merck, Germany) for 10 minutes at room temperature. The PFA was then aspirated, and the cells were washed with 200 μL of PBS.

The cell borders were stained with 100 μL of rhodamine-phalloidin (1:50, Thermo Fisher Scientific, USA) for 15 minutes, dissolved in PBS with 0.2% Triton-X100. After the staining solution was removed, the residual dye was washed away with 200 μL of PBS. Subsequently, the cell nuclei were stained with 100 μL of 4',6-diamidino-2-phenylindole (DAPI, 1:5000, Invitrogen, USA) for 5 minutes, and then the DAPI solution was removed. Finally, the inserts were cut, mounted on glass slides, and stored at 4°C until to use. All procedures were performed in the dark, and images were captured.

Cellular Internalization of NPs

To investigate the internalization of NPs by cells, SW480 cells were seeded at a density of 50,000 cells/mL in 24-well plates and incubated at 37°C for 7 days. After this period, the cells were treated with fluorescently labelled NPs and QU-Free for 4 hours, using the same concentrations as in the Caco-2 cell assay. Following incubation, the medium was discarded, and the wells were washed 3 times with PBS. The SW480 cells were then fixed with 500 μL of 4.5% paraformaldehyde (PFA) for 10 minutes at room temperature. After removing the PFA, the cells were washed with 200 μL of PBS.

The cell borders were stained with 100 μL of rhodamine-phalloidin (1:50) in buffered PBS containing 0.2% Triton-X100 for 15 minutes. Excess dye was washed away with 200 μL of PBS. Next, the cell nuclei were stained with 100 μL of DAPI (1:5000) for 5 minutes, followed by a rinse with PBS. Finally, 500 μL of PBS was added to each well, and images were captured using a confocal microscope. All procedures were performed in the dark.

Animal Experiments

Animals

Eight to ten-week female C57BL/6 mice, weighing 17–21 g, were obtained from Jackson Laboratory. The mice were kept in specific pathogen-free (SPF) conditions, with a 12-hour light-dark cycle at $23 \pm 1^\circ\text{C}$ and $50 \pm 5\%$ humidity. They had unlimited access to water and standard lab chow. Health checks were routinely conducted by a veterinarian to monitor for microbial and parasitic infections. The mice were acclimated for 5 days before the study. All procedures were approved by the government of Middle Franconia, Germany, and adhered to institutional guidelines (approval number 55.2.2–2532-2-1152-18).

Positive Control Group Establishment and Dose Rationale

In accordance with established protocols for quercetin efficacy studies in IBD models, we implemented a dose-stratified positive control system using QU-Free. Based on literature demonstrating that 50–100 mg/kg/day (approximately 1–2 mg/day for 20g mice) represents the effective dose for colitis treatment in C57BL/6 mice, we designed: (1) a high-dose positive control group (QU-Free 3 mg/day, equivalent to 150 mg/kg/day) to ensure robust therapeutic effects; and (2) a low-dose group (QU-Free 1 mg/day) to evaluate baseline efficacy.^{12,13} The nanoformulation treatment groups (QU-PLGA and QU-PE) received 1 mg/day to directly compare their therapeutic potential against both conventional quercetin

doses and disease controls. This tiered approach allows comprehensive evaluation of dose-response relationships and nanoparticle-enhanced bioavailability.

Acute Dextran Sulfate Sodium Salt (DSS)-Induced Colitis Model

Acute colitis was induced by 3%DSS (36–50kD; MP Biotech, Santa Ana, CA, United States) to drinking water of mice (4 mice per group). Mice were identified, weighed, and monitored daily. On day 9, colitis severity was assessed via mini endoscopy (Karl Storz, Germany), followed by euthanasia for colorectal tissue analysis.

Acute Oxazolone (OXA)-Induced Colitis Model

To induce inflammation as an acute colitis model, mice were sensitized with 100 μ L of 3% OXA (Sigma-Aldrich, USA) (in 4:1 acetone-olive oil) on their shaved abdomens (4 mice per group). Mice were tagged, weighed, and observed daily. Five days later, under anesthesia with 100 μ L Ketamine/Xylazine PBS, 100 μ L of 1% oxazolone in 50% ethanol was administered into the colon via a flexible tube inserted through the anus. Colitis severity was assessed 24 hours later using mini endoscopy, and mice were euthanized 48 hours post-challenge for further analysis.

Murine Endoscopic Index of Colitis Severity (MEICS)

We assessed colonic inflammation in anesthetized mice (2% isoflurane) using mini endoscopy. Five parameters—transparency, granularity, vascularity, stool, and fibrin—were scored from 0 to 3. The score of MEICS ranges from 0 (no inflammation) to 15 (severe inflammation).¹⁴

Histological Evaluation

Colon tissues from mice were embedded in Tissue Tek (Sakura, USA), flash-frozen using liquid nitrogen, and stored at -20°C . Cryosections were cut with a cryostat (Leica CM, Germany), placed on slides, and stored at -80°C . After H&E staining, tissue damage and inflammatory cell infiltration were assessed, with scores ranging from 0–4 for OXA colitis and 0–6 for DSS colitis.¹⁵

Evaluation of MPO Activity Using IVIS

We assessed MPO activity in vivo after endoscopy during DSS or OXA colitis. MPO in neutrophils and macrophages converts H₂O₂ and chloride ions into hypochlorous acid, which reacts with luminol to produce luminescence. Mice were injected with 100 μ L of 20nM luminol L-012 (Sigma-Aldrich, USA), anesthetized with 2% isoflurane, and positioned in the IVIS chamber to measure luminescence for 1 minute.

MPO/E-Cadherin Tissue Staining

Cryosections were fixed with 4.5% PFA for 15 minutes, washed with PBS, and permeabilized with 1 \times permeabilization buffer for 10 minutes. Tissues were then blocked for 30 minutes and stained overnight at 4 $^{\circ}\text{C}$ with primary antibody (MPO staining, 1:50, #AF3667, R&D Systems, USA; E-cadherin staining, #3195S, Cell Signal Technology). Next day, slides were washed and incubated with secondary antibody (MPO 2nd antibody: Rabbit anti-goat Alexa Fluor488 IgG, 1:500, #A11078, Invitrogen, USA; E-cadherin staining: #A11008, Invitrogen, USA) for 2 hours at room temperature. After washing, tissues were stained with DAPI (1:5000) for 5 minutes, mounted with Mowiol (Sigma-Aldrich, USA), and imaged using a confocal microscope. Positive and negative controls were included: negative controls incubated with PBS, and positive controls with PBS and secondary antibodies.

RT-qPCR

Total RNA was extracted from murine colonic tissues and used to synthesize cDNA with the Nucleo Spin RNA kit (Machery Nagel, Germany). The cDNA was stored at -20°C , then diluted and subjected to qPCR using a CFX96 Real-Time System qPCR machine (Bio-Rad, USA). Assay for IL-1 β , IL-6, TNF- α and the housekeeping gene 18s (Qiagen, Germany) were used, and mRNA levels were quantified using the $2^{-\Delta\Delta\text{Ct}}$ method.

Statistics

Data were analyzed with GraphPad Prism 10.0.2. ANOVA was used for comparisons among multiple groups. Results are shown as mean \pm SD. Statistical significance was set at $p < 0.05$, with asterisks indicating significance levels (* < 0.05 , ** < 0.01 , *** < 0.001 , **** < 0.0001).

Results

Characteristics of QU-PLGA and QU-PE

As shown in Table 1 and Figure 1A, the mean particle size of the QU-Free suspension is 2239 ± 404 nm, which is significantly larger than the particle size of QU-PLGA (160.4 ± 3.68 nm) or QU-PE (161.0 ± 2.30 nm). QU-PLGA (-22.1 ± 0.971 mV) or QU-PE (-26.3 ± 0.806 mV) exhibits better stability in aqueous solutions compared to QU-Free (-15.9 ± 1.040 mV). QU-PLGA or QU-PE exhibits a high encapsulation efficiency, ranging from 87% to 90%. Figure 1B shows the solution color characteristics of quercetin-loaded NPs, as well as some of the main instruments used in the preparation process. The SEM images show the morphology of QU-PLGA or QU-PE as microspheres (Figure 1C). The prepared QU-PLGA and QU-PE demonstrated significantly smaller particle sizes and better stability compared to QU-Free. Both formulations showed high EE and spherical morphology under SEM. These optimal physicochemical characteristics indicate successful nanoformulation of quercetin with improved aqueous stability.

Drug Release and Cytotoxicity of Quercetin-Loaded NPs

The drug release of QU-PLGA or QU-PE was evaluated in PBS at pH 7.3 over a 24-hour period. QU-PLGA or QU-PE exhibited a rapid drug release within the first hour, followed by a gradual and sustained release. As depicted in Figure 2A, QU-PLGA showed an initial burst release of around 42%, followed by a cumulative release reaching approximately 62%. Meanwhile, QU-PE exhibited an initial release of roughly 46%, with a total release of about 69%. Furthermore, the in vitro drug release was conducted in a pH gradient medium over 24 hours to simulate the degradation of NPs in the gastrointestinal tract (Figure 2B). The initial pH in PBS was maintained at 1.2 for 2 hours, followed by adjustment to 7.4 for the remaining duration (2 to 24 hours). QU-PE exhibited pH-dependent release profile with a slow release observed at pH 1.2 (approximately 35% release) and a rapid release at pH 7.4 (approximately 92% release). In contrast, quercetin released from QU-PLGA showed no significant pH-dependent effect, reaching approximately 73% release in pH 1.2 medium, and achieving an overall cumulative release of approximately 86%. Drug release profiles revealed distinct behaviors: QU-PE demonstrated pH-responsive release with minimal gastric release and rapid intestinal release, while QU-PLGA showed pH-independent sustained release.

To evaluate the safety of quercetin-loaded NPs, the cytotoxicity of QU-Free, QU-PLGA and QU-PE was examined via the MTT assay. Caco-2 and SW480 cell lines were used to evaluate cytotoxicity at equivalent drug concentrations ranging from 1 to $40\mu\text{M}$. Comparisons were made between the control groups (including medium without quercetin, blank PLGA NPs and blank PE NPs) and the experimental groups (containing QU-Free, QU-PLGA NPs and QU-PE NPs). The incubation concentrations of blank PLGA NPs and blank PE NPs were adjusted to match the equivalent concentrations of the corresponding quercetin-loaded NPs. Figure 2C and D showed the effects of QU-Free and quercetin-loaded NPs on cell viability of Caco-2 or SW480 cells. Regardless of Caco-2 or SW480, the cell viability of the control group was approximately 100%, indicating that blank PLGA NPs or blank PE NPs were non-toxic to the cells. Additionally, the impact of quercetin-loaded NPs on cell viability was not significantly different from that of QU-

Table 1 Physicochemical Characteristic of Quercetin and Its NPs

Drug	Size (nm)	Polydispersity Index	Zeta Potential (mV)	EE (%)
QU-Free	2239 ± 404	0.98 ± 0.024	-15.9 ± 1.040	
QU-PLGA	160.4 ± 3.68	0.030 ± 0.018	-22.1 ± 0.971	90 ± 2.5
QU-PE	161.0 ± 2.30	0.049 ± 0.023	-26.3 ± 0.806	87 ± 2.0

Abbreviations: NPs, nanoparticles; QU-Free, free quercetin; QU-PLGA, quercetin encapsulated in PLGA; QU-PE, quercetin encapsulated in both PLGA and ES100; EE, encapsulation efficiency.

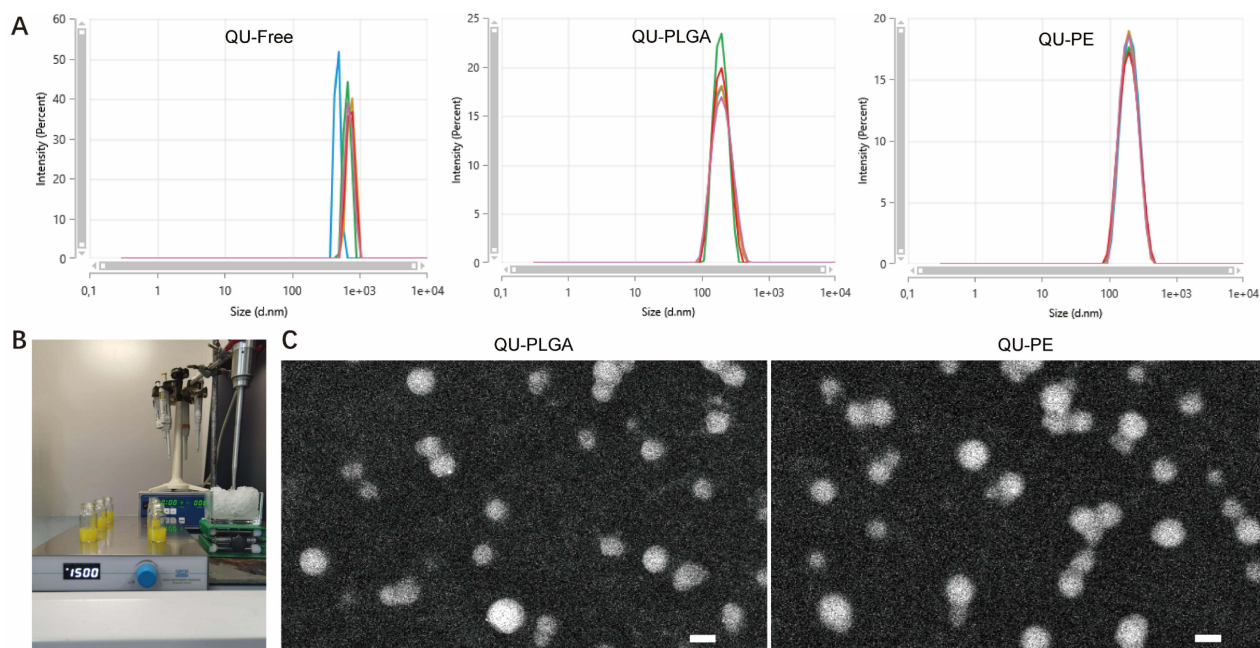


Figure 1 Size and morphology of QU-PLGA and QU-PE. **(A)** Size of QU-Free and NPs; **(B)** Production of NPs; **(C)** Morphology of NPs (Scale bar = 100nm). **Abbreviations:** NPs, nanoparticles; QU-Free, free quercetin; QU-PLGA, quercetin encapsulated in PLGA; QU-PE, quercetin encapsulated in both PLGA and ES100.

Free. Both QU-PLGA and QU-PE showed excellent biocompatibility, showing no cytotoxicity in Caco-2 and SW480 cells at tested concentrations, with cell viability comparable to QU-Free and blank NPs controls.

Cellular Penetration and Permeability of NPs

The cellular uptake of coumarin 6-labeled QU-Free and quercetin-loaded NPs was investigated through cell endocytosis assay in SW480 cells. In the [Figure 3A](#), it can be observed that QU-PLGA or QU-PE penetrates partially through the cell membrane and enters into SW480 cells after 4 hours of incubation, whereas free quercetin was not detected inside the cells. This suggests that quercetin-loaded NPs exhibit enhanced capability to cross the cell membrane compared to QU-Free.

To assess the permeability of quercetin-loaded NPs across the intestinal barrier, Caco-2 cell monolayers were utilized as a model for the intestinal epithelium. QU-PLGA or QU-PE did not show significant accumulation within the Caco-2 cell monolayers, whereas QU-Free of different sizes exhibited marked aggregation within these cell layers. This indicates that QU-PLGA or QU-PE can traverse the intestinal epithelial barrier more effectively compared to QU-Free ([Figure 3B](#)).

Both QU-PLGA and QU-PE demonstrated superior cellular penetration in SW480 cells and enhanced intestinal permeability in Caco-2 monolayers compared to QU-Free, confirming that NP encapsulation improves quercetin's bioavailability.

Animal Assays

Therapeutic Benefits of Quercetin-Loaded NPs in the DSS-Induced Acute Colitis

In the DSS-induced acute colitis model, the mice were randomly divided into the following groups: DSS group (100 μ L of tap water daily), low-dose group (1 mg of quercetin daily), high-dose group (3 mg of quercetin daily), QU-PLGA group (QU-PLGA solution containing 1 mg of quercetin daily), and QU-PE group (QU-PE solution containing 1 mg of quercetin daily). One mouse in the DSS group died from acute colitis while one mouse in the low-dose group died from aspiration due to improper initial gavage. [Figure 4A](#) showed that mice in both the DSS and low-dose groups on day 7 displayed significant anal bleeding, while those in the high-dose, QU-PLGA, and QU-PE groups exhibited no signs of

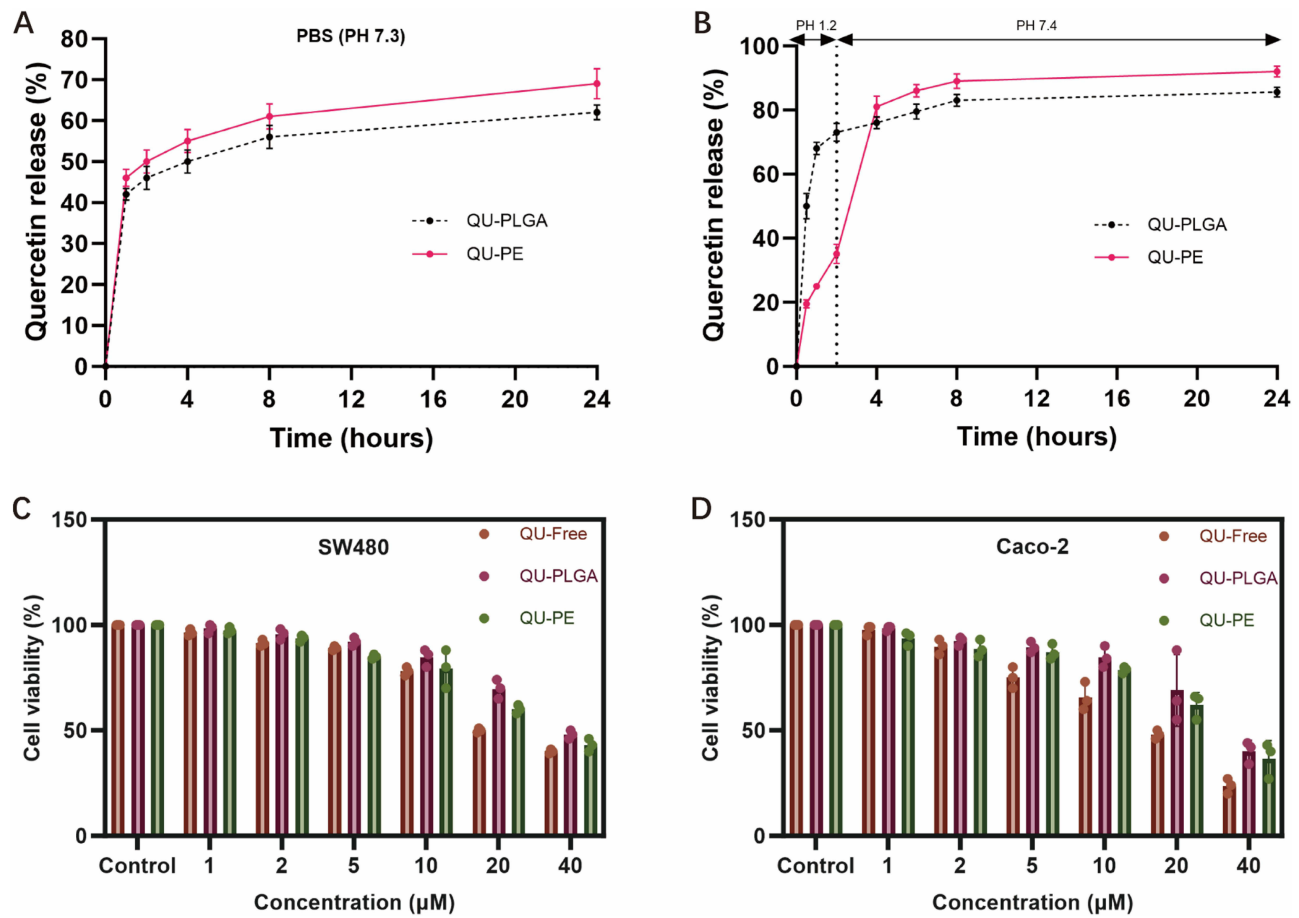


Figure 2 In vitro drug release and cytotoxicity assay of QU-PLGA and QU-PE. (A) in vitro drug release of NPs at pH = 7.3; (B) in vitro drug release of NPs at pH = 1.2 and pH = 7.4; (C) Cytotoxicity assay of NPs for SW480; (D) Cytotoxicity assay of NPs for Caco-2.

Abbreviations: NPs, nanoparticles; QU-Free, free quercetin; QU-PLGA, quercetin encapsulated in PLGA; QU-PE, quercetin encapsulated in both PLGA and ES100.

anal bleeding. The colon length of mice in the DSS group was significantly shorter than that in the high-dose and QU-PLGA groups. Although the colon length in the QU-PE and low-dose groups was longer than that in the DSS group, the difference was not statistically significant (Figure 4B and C).

Figure 5A illustrated the experimental timeline for DSS-induced acute colitis. The high-dose group, QU-PLGA group, and QU-PE group of mice experienced a slower rate of weight loss compared to the DSS group. But there was no statistically difference in weight loss between the low-dose group and the DSS group of mice (Figure 5B). IVIS experiment showed that the luminescence emission intensity of mice in the low-dose, high-dose, QU-PLGA, and QU-PE groups was lower than that of mice in the DSS group (Figure 5C). Through endoscopic examination, we found that the intestinal MEICS scores of mice in the low-dose, high-dose, QU-PLGA, and QU-PE groups were lower than those in the DSS group (Figure 5D). The histological scores of the colon in DSS group were higher than the other four groups. However, no statistically difference in histological scores was observed between the DSS group and the low-dose group (Figure 5E). Compared to the low-dose, high-dose, QU-PLGA, and QU-PE groups, mice in the DSS group exhibited higher number of MPO-positive cells in colon tissues (5F). To evaluate the extent of colon epithelial barrier disruption, E-cadherin antibody staining was performed on colon tissues (Figure 5G). We found that E-cadherin fluorescence intensity of the colon epithelium in the high-dose, QU-PLGA, and QU-PE groups was significantly stronger than in the DSS group, and the low-dose group exhibited slightly stronger intensity than the DSS group, which indicates that high-dose quercetin, PLGA-encapsulated quercetin, and PE-encapsulated quercetin provide protective effect on the colon epithelial barrier in mice. Additionally, the high-dose and QU-PLGA groups exhibited lower mRNA levels of IL6 and higher mRNA levels of IL10 compared to the DSS group. TNF α mRNA expression in the colon tissues of mice in the high-dose group, QU-PLGA group or QU-PE group was lower than that in the DSS group (Figure 5H).

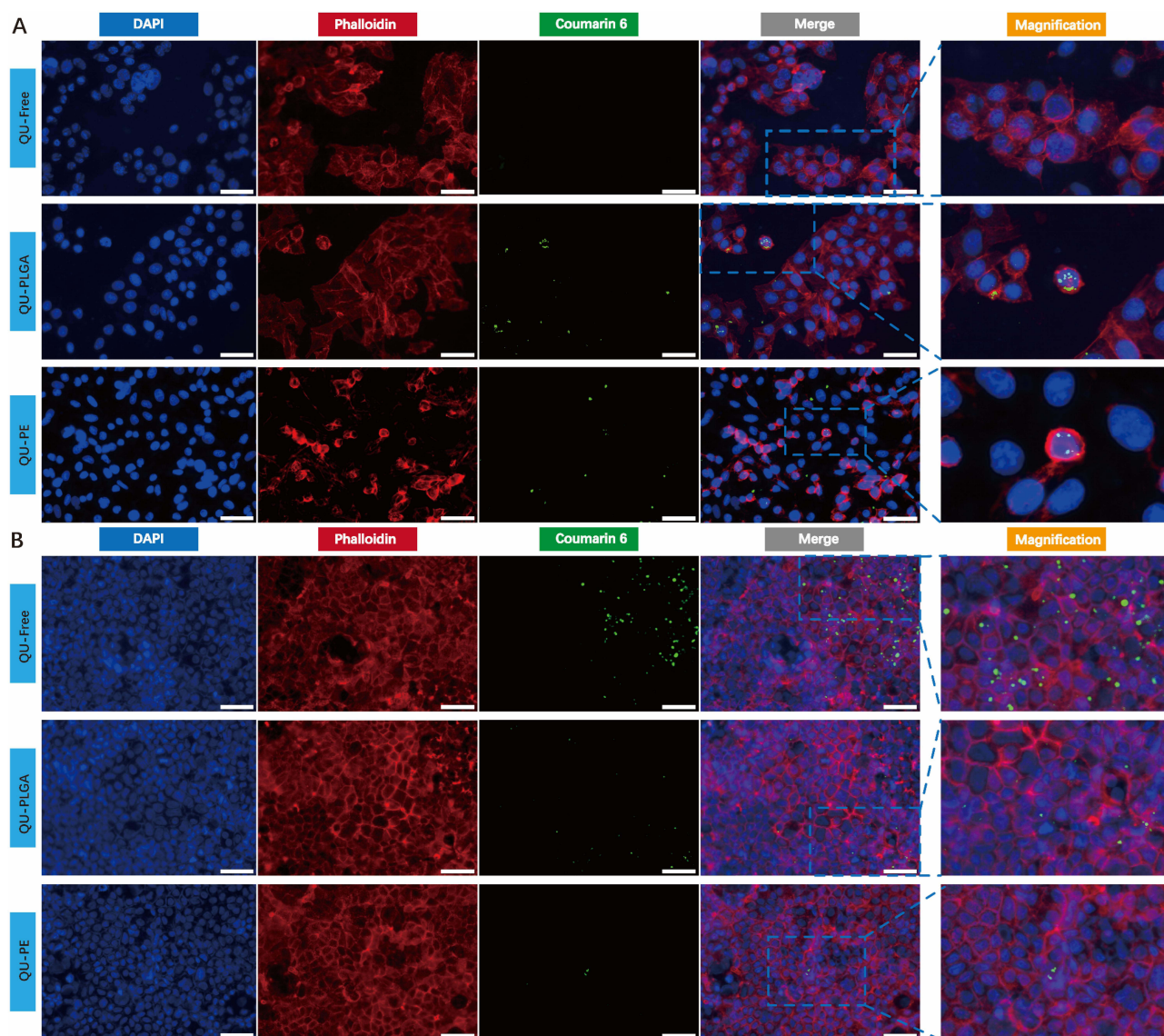


Figure 3 Cell endocytosis and permeability of QU-Free and quercetin-loaded NPs. (A) Cell endocytosis assay (Scale bar = 50 μ m); (B) Permeability assay (Scale bar = 50 μ m).

Abbreviations: NPs, nanoparticles; QU-Free, free quercetin; QU-PLGA, quercetin encapsulated in PLGA; QU-PE, quercetin encapsulated in both PLGA and ES100.

In the DSS-induced colitis model, both QU-PLGA and QU-PE showed marked therapeutic effects in DSS-induced colitis compared to controls. While both formulations improved inflammation and epithelial repair, QU-PLGA appeared more potent in inflammation control.

Protective Effects of Quercetin-Loaded NPs in the OXA-Induced Acute Colitis

In the model of acute colitis induced by OXA, mice were randomly categorized into five groups: OXA group (100 μ L of tap water administered daily), low-dose group (daily administration of 1 mg quercetin), high-dose group (daily administration of 3 mg quercetin), QU-PLGA group (daily administration of QU-PLGA containing 1 mg quercetin), and QU-PE group (daily administration of QU-PE containing 1 mg quercetin). Figure 6A depicted the established timeline of an OXA-induced acute colitis model. From the 1st day after the challenge, mice in the OXA group exhibited the most significant weight loss, which was statistically significant compared to the high-dose and PE groups. However, there was no statistical difference in weight loss between the OXA group and the QU-PLGA or low-dose groups of mice (Figure 6B). The IVIS experiment showed that the luminescence intensity in the OXA group was significantly higher than that in the low-dose group, high-dose group, QU-

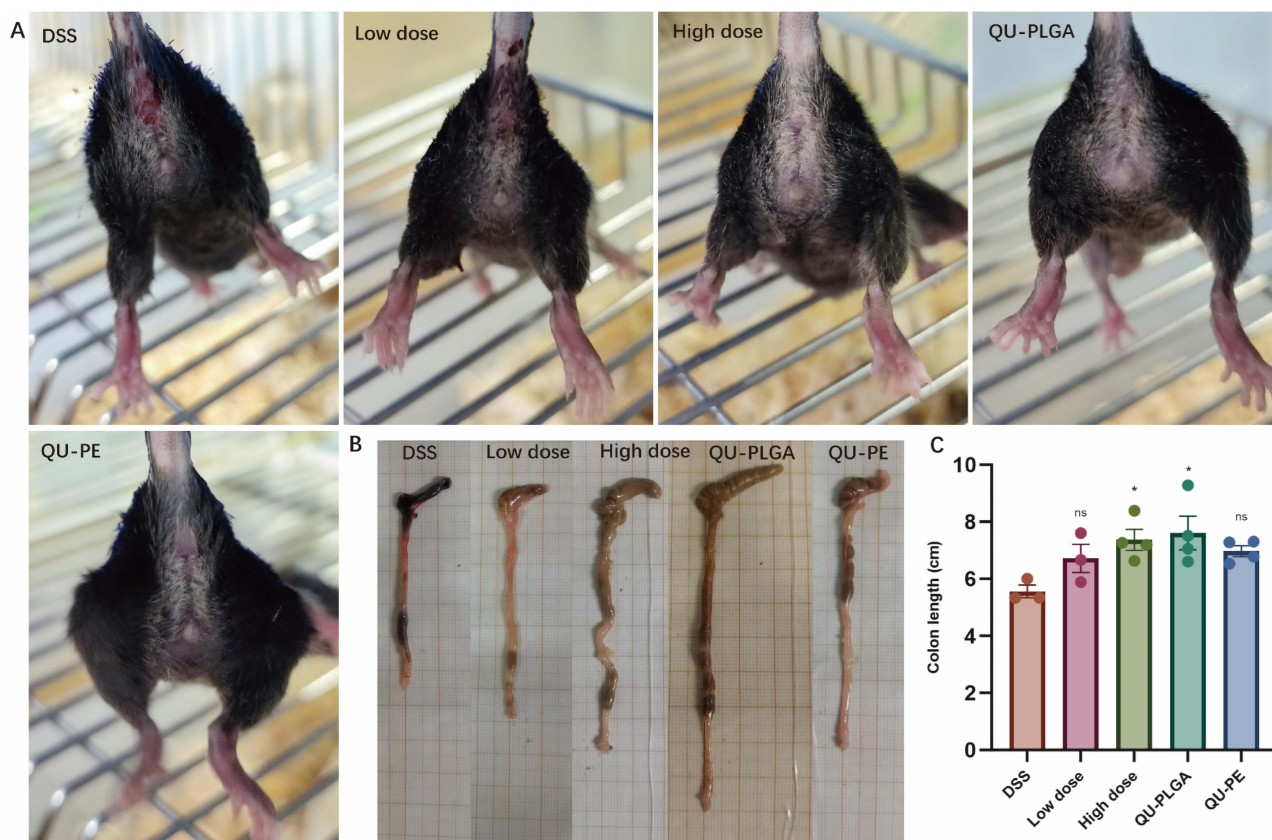


Figure 4 Anal bleeding conditions and colon length change of different groups in the DSS-induced acute colitis model. **(A)** Representative image showing anal bleeding on day 7; **(B)** Macroscopic assessment of colon shortening; **(C)** Quantitative analysis of colon length.

Abbreviations: DSS, dextran sulfate sodium salt; QU-PLGA, quercetin encapsulated in PLGA; QU-PE, Quercetin encapsulated in both PLGA and ES100. ns: > 0.05, * < 0.05.

PLGA group, and QU-PE group (Figure 6C). The MEICS score of the colon through endoscopic examination in the OXA group of mice was higher than that in the high-dose group, QU-PLGA group, and QU-PE group. However, there was no significant difference in the colonic MEICS score between the OXA group and the low-dose group of mice (Figure 6D). In the OXA colitis model, the histological scores of the colon in the high-dose group and QU-PE group were lower than those in the OXA group. However, the colonic histological scores in the QU-PLGA group and low-dose group did not show a significant reduction compared to the OXA group (Figure 6E). The colonic tissue of mice in the OXA group or low-dose group contained more MPO-positive cells compared to the high-dose group, QU-PLGA group or QU-PE group (Figure 6F). Similarly, we found that the colonic epithelium cells of mice in the low-dose group, high-dose group, QU-PLGA group, and QU-PE group had higher E-cadherin expression than those in the OXA group (Figure 6G). In addition, compared to the OXA group, the expression of IL-6 and TNF- α in the colonic tissue of mice in the high-dose group and QU-PE group was lower, while the expression of IL-10 in the colonic tissue of mice in the QU-PE group was highest among all groups. QU-PE group had higher IL1 β mRNA expression than OXA group. QU-PLGA group was identified to have higher TNF α mRNA expression compare to OXA group (Figure 6H).

In the OXA-induced colitis model, both nanoformulations presented therapeutic benefits, but QU-PE demonstrated optimal efficacy in ameliorating weight loss, inflammation, and epithelial damage compared to QU-PLGA.

Discussion

IBD is typically managed through the use of anti-inflammatory drugs, immunosuppressants, and biologics, each with varying degrees of success and associated side effects such as increased infection risk, liver toxicity, and gastrointestinal discomfort. Despite these treatments, many patients experience relapses or incomplete symptom control, highlighting the

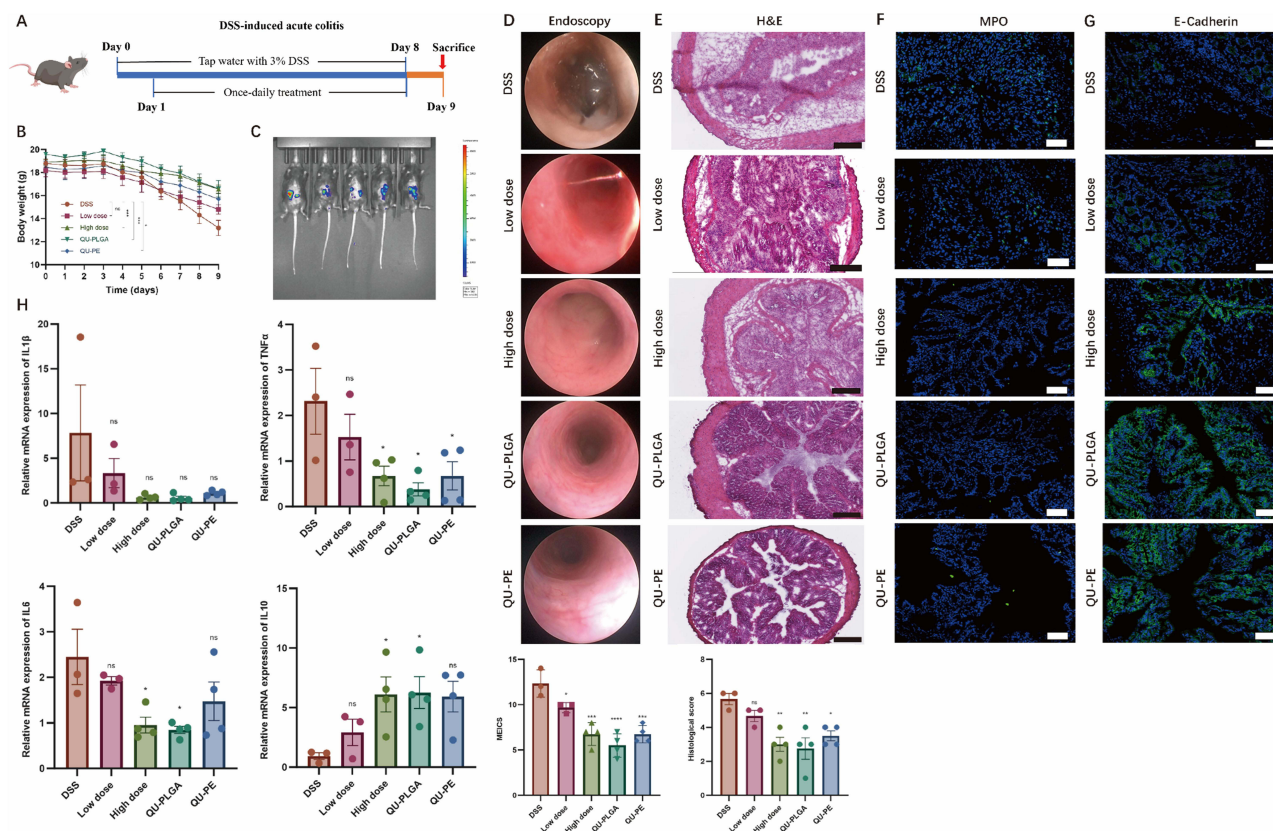


Figure 5 Therapeutic efficacy of quercetin and its NPs in the DSS-induced acute colitis. **(A)** Treatment timeline; **(B)** Weight change; **(C)** IVIS; **(D)** Endoscopic examination; **(E)** H&E staining (Scale bar = 250 μ m); **(F)** MPO staining (Scale bar = 50 μ m); **(G)** E-cadherin staining (Scale bar = 50 μ m); **(H)** RT-qPCR.

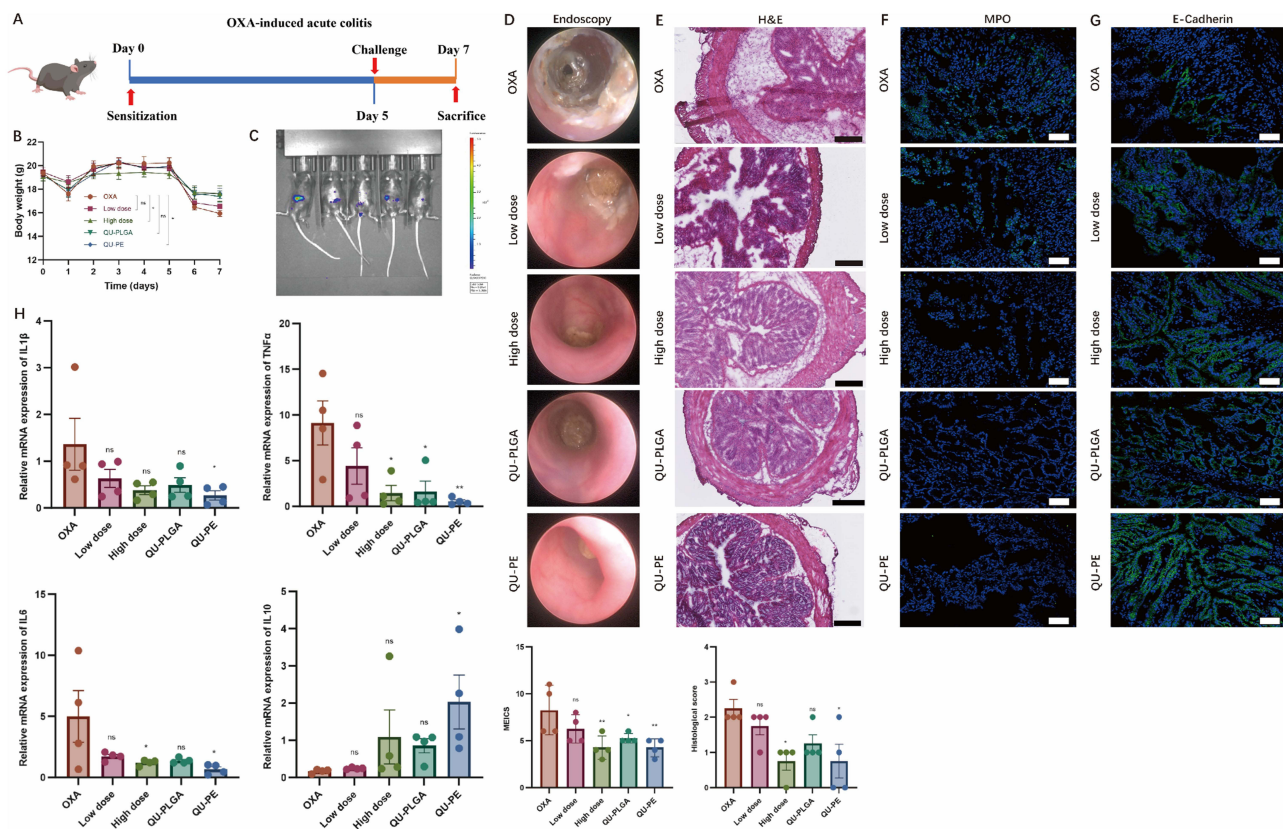
Abbreviations: NPs, nanoparticles; DSS, dextran sulfate sodium salt; QU-PLGA, quercetin encapsulated in PLGA; QU-PE, quercetin encapsulated in both PLGA and ES100; MPO, myeloperoxidase; IVIS, in vivo imaging system. ns: > 0.05, * < 0.05, ** < 0.01, *** < 0.001, **** < 0.0001.

need for more effective and safer therapeutic options. In this study, the encapsulation of quercetin with PLGA or PE presents a novel approach that not only enhances the therapeutic efficacy of quercetin—a bioflavonoid with known anti-inflammatory and antioxidant properties—but also improves its stability and bioavailability, offering a promising alternative for IBD treatment.

The mean particle size of QU-Free suspension was observed to be significantly larger compared to QU-PLGA or QU-PE. The reduction in particle size upon encapsulation is a critical factor that enhances the bioavailability and cellular uptake of quercetin, as smaller particles are known to have a larger surface area for absorption and interaction with biological membranes.^{16,17} Moreover, the stability of quercetin in aqueous solutions was markedly improved when encapsulated, as indicated by the more negative zeta potential values compared to QU-Free. Stability in aqueous solutions is paramount for the effective delivery of quercetin in biological systems, where rapid degradation and poor solubility are significant challenges.¹⁸

The in vitro drug release profile of quercetin-loaded NPs exhibited a rapid initial burst followed by a sustained release, which is beneficial for achieving immediate therapeutic effects followed by prolonged action. Specifically, QU-PLGA showed an initial burst release of approximately 42% and a cumulative release of 62%, while QU-PE had an initial release of around 46% and a total release of about 69%. The pH-dependent release profile of PE NPs, with slower release at pH 1.2 and rapid re-lease at pH 7.4, aligns with the gastrointestinal environment, where QU-PE can protect quercetin in the acidic stomach and release it in the more neutral intestines.¹⁹ This targeted release mechanism enhances the bioavailability and effectiveness of quercetin, particularly for gastrointestinal applications.

The enhanced cellular uptake of QU-PLGA or QU-PE compared to QU-Free is significant, as demonstrated by cell endocytosis assays with SW480 cells. Encapsulated quercetin penetrated the cell membrane more effectively, likely due



to the smaller particle size and increased stability of the NPs.¹⁸ This improved cellular uptake is crucial for maximizing the therapeutic effects of quercetin, especially in cancer cells or inflamed tissues where higher intracellular concentrations are needed. Additionally, the superior permeability of quercetin-loaded NPs across Caco-2 cell monolayers further supports their potential for oral administration, where efficient absorption through the intestinal barrier is essential.²⁰

The therapeutic efficacy of quercetin-loaded NPs was evident in the DSS-induced acute colitis model. Mice treated with high-dose quercetin, QU-PLGA, or QU-PE exhibited reduced symptoms of colitis, such as less anal bleeding, slower weight loss, and longer colon length. These groups also showed lower MEICS and histological scores, indicating less severe colonic damage and inflammation. The reduced luminescence emission intensity and fewer MPO-positive cells in these groups suggest decreased neutrophil infiltration and oxidative stress, which are key factors in IBD. In the OXA-induced acute colitis, similar therapeutic benefits were observed. Mice treated with high-dose quercetin or QU-PE had significantly less weight loss and lower MEICS and histological scores compared to the OXA group. The reduced expression of pro-inflammatory cytokines IL-6 and TNF- α , along with increased IL-10 levels, highlights the anti-inflammatory effects of quercetin-loaded NPs. The enhanced E-cadherin expression in treated groups further indicates better maintenance of the intestinal epithelial barrier, which is critical for preventing disease progression in IBD. At present, multiple studies have confirmed that quercetin loaded NPs have anti-inflammatory effects and can alleviate intestinal inflammation in mice.^{21,22}

Comparative analysis revealed distinct therapeutic profiles between the nanoformulations: QU-PE exhibited stable anti-inflammatory activity in both experimental systems, displaying especially marked therapeutic benefits in OXA-induced colitis (including better weight stability, improved endoscopic scores, and enhanced mucosal barrier function). Conversely, QU-PLGA manifested comparatively better treatment outcomes in the DSS model (particularly regarding colon length conservation and cytokine modulation). This differential efficacy can be mechanistically explained by their

distinct delivery characteristics, consistent with Meissner et al's comparative study of PLGA versus pH-sensitive NPs (Eudragit P-4135F) in IBD.²³ While pH-sensitive NPs demonstrate reduced inflamed tissue targeting but higher total drug delivery to the colon, PLGA NPs show selective accumulation in inflammatory lesions despite lower total drug amounts. In OXA-induced colitis featuring focal distal inflammation, QU-PE's pH-dependent release likely reduced proximal intestinal drug deposition while enhancing delivery to affected distal colon regions. Conversely, in DSS-induced colitis with diffuse lesions, QU-PE's lack of targeted accumulation may limit efficacy, whereas QU-PLGA's preferential inflammation targeting proves advantageous for widespread colonic involvement.

The findings of this study are consistent with previous research on the benefits of NP encapsulation for enhancing the bioavailability and therapeutic effects of quercetin.^{13,24} Similar improvements in stability, cellular uptake, and controlled release have been reported for other encapsulated flavonoids and polyphenols.²⁵ The use of PLGA and ES100 as encapsulating materials is particularly advantageous due to their biocompatibility, biodegradability, and FDA approval for drug delivery applications.²⁶

While our findings demonstrate promising therapeutic effects of quercetin-loaded NPs in acute colitis models, several limitations should be acknowledged. First, the current study only validated NP efficacy in the acute colitis model, leaving their therapeutic potential in chronic IBD models unexplored—an important consideration given the recurrent nature of human IBD. Second, critical pharmacokinetic parameters including biodistribution profiles, organ accumulation patterns, and systemic clearance mechanisms of the NPs remain uncharacterized. Third, as noted earlier, the absence of clinical data and long-term toxicity evaluation presents a significant translational gap. Future studies should specifically address these limitations by: (1) evaluating NP performance in chronic colitis models (eg, multiple-cycle DSS or IL-10 knockout mice) to assess durability of treatment effects; (2) conducting comprehensive biodistribution studies using fluorescent/radioactive labeling to track NP fate *in vivo*; and (3) establishing pharmacokinetic-pharmacodynamic relationships through serial blood/tissue sampling. These investigations will be essential for determining optimal dosing regimens and potential off-target effects before clinical translation.

Conclusion

In summary, the encapsulation of quercetin with PLGA or PE significantly enhances its stability, bioavailability, and therapeutic efficacy. The controlled release profiles, improved cellular uptake, and permeability, along with the demonstrated benefits in animal models of acute colitis, underscore the potential of quercetin-loaded NPs as a promising therapeutic strategy for IBD and other conditions where quercetin's bioactivity can be leveraged. Future research should focus on clinical trials to validate these findings and explore the broader applications of quercetin-loaded NPs in human health.

Data Sharing Statement

The data supporting this study are not openly available but can be requested from the author for scholarly purposes.

Ethical Recognition

The animal ethics approval for this study was granted by the Government of Middle Franconia, Germany, and the procedures adhered to the institutional guidelines (approval number 55.2.2-2532-2-1152-18). The ethical approval document is available upon request.

Consent for Publication

All authors agree to publish.

Author Contributions

All authors made a significant contribution to the work reported, whether that is in the conception, study design, execution, acquisition of data, analysis and interpretation, or in all these areas; took part in drafting, revising or critically reviewing the article; gave final approval of the version to be published; have agreed on the journal to which the article has been submitted; and agree to be accountable for all aspects of the work.

Funding

This study was supported by the IZKF (A103) by University Erlangen, Tianjin Key Medical Discipline (Specialty) Construction Project (Grant No. TJYXZDXK-009A), Tianjin Medical University Cancer Hospital National Natural Science Foundation Cultivation Program (Grant No. 220108), and China Scholarship Council (CSC) (Grant No. 202208610036).

Disclosure

The authors declare no conflicts of interest in this work.

References

- Bruner LP, White AM, Proksell S. Inflammatory bowel disease. *Prim Care*. 2023;50(3):411–427. doi:10.1016/j.pop.2023.03.009
- Adolph TE, Meyer M, Schwärzler J, Mayr L, Grabherr F, Tilg H. The metabolic nature of inflammatory bowel diseases. *Nat Rev Gastroenterol Hepatol*. 2022;19(12):753–767. doi:10.1038/s41575-022-00658-y
- Takahashi S, Muguruma H, Osakabe N, Inoue H, Ohsawa T. Electrochemical determination with a long-length carbon nanotube electrode of quercetin glucosides in onion, apple peel, and tartary buckwheat. *Food Chem*. 2019;300:125189. doi:10.1016/j.foodchem.2019.125189
- Hu S, Zhao M, Li W, et al. Preclinical evidence for quercetin against inflammatory bowel disease: a meta-analysis and systematic review. *Inflammopharmacology*. 2022;30(6):2035–2050. doi:10.1007/s10787-022-01079-8
- Zhang Q, Wen F, Sun F, et al. Efficacy and mechanism of quercetin in the treatment of experimental colitis using network pharmacology analysis. *Molecules*. 2022;28(1):146. doi:10.3390/molecules28010146
- Zhu X, Li Y, Yue L, et al. Quercetin mitigates radiation-induced intestinal injury and promotes intestinal regeneration via Nrf2-mediated antioxidant pathway1. *Radiat Res*. 2023;199(3):252–262. doi:10.16667/RADE-22-00090.1
- Liu T, Fan S, Meng P, et al. Dietary dihydroquercetin alleviated colitis via the short-chain fatty acids/miR-10a-5p/PI3K-Akt signaling pathway. *J Agric Food Chem*. 2024;72(42):23211–23223. doi:10.1021/acs.jafc.4c03278
- Li Y, Yao J, Han C, et al. Quercetin, Inflammation and Immunity. *Nutrients*. 2016;8(3):167. doi:10.3390/nu8030167
- Rahmani F, Naderpour S, Nejad BG, et al. The recent insight in the release of anticancer drug loaded into PLGA microspheres. *Med Oncol*. 2023;40(8):229. doi:10.1007/s12032-023-02103-9
- Naem M, Kim W, Cao J, Jung Y, Yoo JW. Enzyme/pH dual sensitive polymeric nanoparticles for targeted drug delivery to the inflamed colon. *Colloids Surf B Biointerfaces*. 2014;123:271–278. doi:10.1016/j.colsurfb.2014.09.026
- Jacob EM, Borah A, Pillai SC, Kumar DS. Garcinol encapsulated Ph-sensitive biodegradable nanoparticles: a novel therapeutic strategy for the treatment of inflammatory bowel disease. *Polymers*. 2021;13(6):862. doi:10.3390/polym13060862
- Topçu-Tarladaçalışır Y, Sapmaz-Metin M, Mercan Z, Erçetin D. Quercetin attenuates endoplasmic reticulum stress and apoptosis in TNBS-induced colitis by inhibiting the glucose regulatory protein 78 activation. *Balkan Med J*. 2024;41(1):30–37. doi:10.4274/balkanmedj.galenos.2023.2023-10-9
- Sun W, Chen Y, Wang L, et al. Gram-scale preparation of quercetin supramolecular nanoribbons for intestinal inflammatory diseases by oral administration. *Biomaterials*. 2023;295:122039. doi:10.1016/j.biomaterials.2023.122039
- Becker C, Fantini MC, Wirtz S, et al. *In vivo* imaging of colitis and colon cancer development in mice using high resolution chromoendoscopy. *Gut*. 2005;54(7):950–954. doi:10.1136/gut.2004.061283
- Wirtz S, Popp V, Kindermann M, et al. Chemically induced mouse models of acute and chronic intestinal inflammation. *Nat Protoc*. 2017;12(7):1295–1309. doi:10.1038/nprot.2017.044
- Chakraborty K, Tripathi A, Mishra S, Mallick AM, Roy RS. Emerging concepts in designing next-generation multifunctional nanomedicine for cancer treatment. *Biosci Rep*. 2022;42(7):BSR20212051. doi:10.1042/BSR20212051
- Li X, Huang Z, Liao Z, Liu A, Huo S. Transformable nanodrugs for overcoming the biological barriers in the tumor environment during drug delivery. *Nanoscale*. 2023;15(19):8532–8547. doi:10.1039/d2nr06621a
- Yin Z, Zheng T, Ho CT, Huang Q, Wu Q, Zhang M. Improving the stability and bioavailability of tea polyphenols by encapsulations: a review. *Food Science and Human Wellness*. 2022;11(3):537–556. doi:10.1016/j.fshw.2021.12.011
- Wang J, Yao M, Zou J, et al. pH-sensitive nanoparticles for colonic delivery anti-miR-301a in mouse models of inflammatory bowel diseases. *Nanomaterials*. 2023;13(20):2797. doi:10.3390/nano13202797
- Chai GH, Xu Y, Chen SQ, et al. Transport mechanisms of solid lipid nanoparticles across Caco-2 cell monolayers and their related cytotoxicology. *ACS Appl Mater Interfaces*. 2016;8(9):5929–5940. doi:10.1021/acsami.6b00821
- Dong Y, Lei J, Zhang B. Dietary quercetin alleviated DSS-induced colitis in mice through several possible pathways by transcriptome analysis. *Curr Pharm Biotechnol*. 2020;21(15):1666–1673. doi:10.2174/1389201021666200711152726
- Diez-Echave P, Ruiz-Malagón AJ, Molina-Tijeras JA, et al. Silk fibroin nanoparticles enhance quercetin immunomodulatory properties in DSS-induced mouse colitis. *Int J Pharm*. 2021;606:120935. doi:10.1016/j.ijpharm.2021.120935
- Meissner Y, Pellequer Y, Lamprecht A. Nanoparticles in inflammatory bowel disease: particle targeting versus pH-sensitive delivery. *Int J Pharm*. 2006;316(1–2):138–143. doi:10.1016/j.ijpharm.2006.01.032
- Jing S, Chen H, Liu E, et al. Oral pectin/oligochitosan microspheres for colon-specific controlled release of quercetin to treat inflammatory bowel disease. *Carbohydr Polym*. 2023;316:121025. doi:10.1016/j.carbpol.2023.121025
- Stevens Barrón JC, Chapa González C, Álvarez Parrilla E, De la Rosa A. Nanoparticle-mediated delivery of flavonoids: impact on proinflammatory cytokine production: a systematic review. *Biomolecules*. 2023;13(7):1158. doi:10.3390/biom13071158
- Makadia HK, Siegel SJ. Poly lactic-co-glycolic acid (PLGA) as biodegradable controlled drug delivery carrier. *Polymers*. 2011;3(3):1377–1397. doi:10.3390/polym3031377

Journal of Inflammation Research

Publish your work in this journal

The Journal of Inflammation Research is an international, peer-reviewed open-access journal that welcomes laboratory and clinical findings on the molecular basis, cell biology and pharmacology of inflammation including original research, reviews, symposium reports, hypothesis formation and commentaries on: acute/chronic inflammation; mediators of inflammation; cellular processes; molecular mechanisms; pharmacology and novel anti-inflammatory drugs; clinical conditions involving inflammation. The manuscript management system is completely online and includes a very quick and fair peer-review system. Visit <http://www.dovepress.com/testimonials.php> to read real quotes from published authors.

Submit your manuscript here: <https://www.dovepress.com/journal-of-inflammation-research-journal>

Dovepress
Taylor & Francis Group